Norman Rostoker and Strongly Correlated Plasmas

Setsuo Ichimaru (Univ. of Tokyo)

OUTLINES AND KEY-PHRASES

Scattering of Electromagnetic Waves by a Strongly Correlated Plasma

- Cross-sections of scattering; structure factors; correlation functions; radar back-scattering from the ionosphere; plasma critical opalescence; Laue patterns with super-cooled Coulomb glasses; ionic quasi-crystals in a laser-cooled non-neutral plasma

Multi-particle Correlation, Equations of State, and Phase Diagrams

- RPA correlation with superposition of dressed test charges; correlation energy beyond RPA; phase diagrams of hydrogen: metallization, solidification, and magnetization; magnetic white dwarfs; phase diagram of nuclear matter

Norman Rostoker and Strongly Correlated Plasmas

Setsuo Ichimaru (Univ. of Tokyo)

SUBJECT HEADING AND MAJOR REFERENCES 1

Scattering of Electromagnetic Waves by a Strongly Correlated Plasma

- S. Ichimaru, D. Pines and N. Rostoker "Observation of critical fluctuations associated with plasma-wave instabilities" Phys. Rev. Lett. **8**, 231 (1962).
- M. N. Rosenbluth and N. Rostoker "Scattering of electromagnetic waves by a nonequilibrium plasma" Phys. Fluids **5**, 776 (1962).
- S. Ogata and S. Ichimaru "Observation of layered structures and Laue patterns in Coulomb glasses" Phys. Rev. Lett. **62**, 2293 (1989).

Norman Rostoker and Strongly Correlated Plasmas

Setsuo Ichimaru (Univ. of Tokyo)

SUBJECT HEADING AND MAJOR REFERENCES 2

Multi-particle Correlation, Equations of State, and Phase Diagrams

- N. Rostoker and M. N. Rosenbluth "Test particles in a completely ionized plasma" Phys. Fluids 3, 1 (1960).
- T. O'Neil and N. Rostoker "Triple correlation for a plasma" Phys. Fluids. 8, 1109 (1965).
- H. Kitamura and S. Ichimaru "Metal-insulator transitions in dense hydrogen: equations of state, phase diagrams and interpretation of shock-compression experiments" J. Phys. Soc. Japan **67**, 950 (1998).
- S. Ichimaru "Ferromagnetic and freezing transitions in charged fermions: Metallic hydrogen" Phys. Plasmas 8, 48 (2001).

Scattering Cross-section

Cross-section of Thomson scattering

$$\sigma_T = \frac{8\pi}{3}\left(\frac{e^2}{mc^2}\right)^2 = 6.553 \times 10^{-25}\ (\mathrm{cm}^2)$$

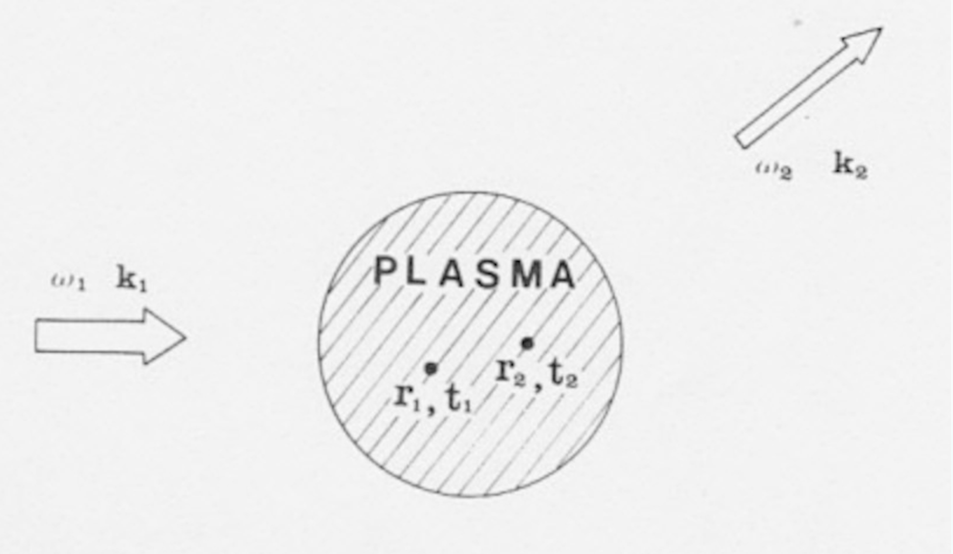

With polarization: η_1, η_2

$$\frac{d^2Q}{do\,d\omega} = \frac{3V}{8\pi}\sigma_T(\hat{\eta}_1 \cdot \hat{\eta}_2)^2 S(\mathbf{k},\omega)$$

where $\mathbf{k} = \mathbf{k}_2 - \mathbf{k}_1$ and $\omega = \omega_2 - \omega_1$.

Without polarization: η_1, η_2

$$\frac{d^2Q}{do\,d\omega} = \frac{3V}{8\pi}\sigma_T\left(1 - \frac{1}{2}\sin^2\theta\right)S(\mathbf{k},\omega)$$

θ is the scattering angle between $\mathbf{k}_1$ and $\mathbf{k}_2$.

DYNAMIC STRUCTURE FACTOR

spectral distribution in **k** and ω of electron density fluctuations

$$S(\mathbf{k},\omega) = \frac{1}{2\pi V}\int_{-\infty}^{\infty} dt \langle \rho_{\mathbf{k}}(t' + t)\rho_{-\mathbf{k}}(t')\rangle \exp(i\omega t) .$$

DYNAMIC STRUCTURE FACTOR

$$S(\mathbf{k},\omega)=\frac{1}{2\pi V}\int_{-\infty}^{\infty}dt\langle\rho_{\mathbf{k}}(t'+t)\rho_{-\mathbf{k}}(t')\rangle\exp(i\omega t)\,.$$

$$\rho_{\mathbf{k}}(t)=\int d\mathbf{r}\left\{\sum_{j=1}^{N}\delta[\mathbf{r}-\mathbf{r}_j(t)]-n\right\}\exp(-i\mathbf{k}\cdot\mathbf{r})$$

$$=\sum_{j=1}^{N}\exp[-i\mathbf{k}\cdot\mathbf{r}_j(t)]-N\delta(\mathbf{k},0)\,,$$

Spectral distribution of density fluctuations for N electrons with trajectories $\mathbf{r}_j(t)$

Fourier transform of density-density correlation between electrons

IONOSPHERIC BACKSCATTERING

IONOSPHERIC F-LAYER

Altitude: 200～500 km

$n = 10^5 - 10^6\ \mathrm{cm}^{-3}$
$T = 1{,}500\ \mathrm{K}$

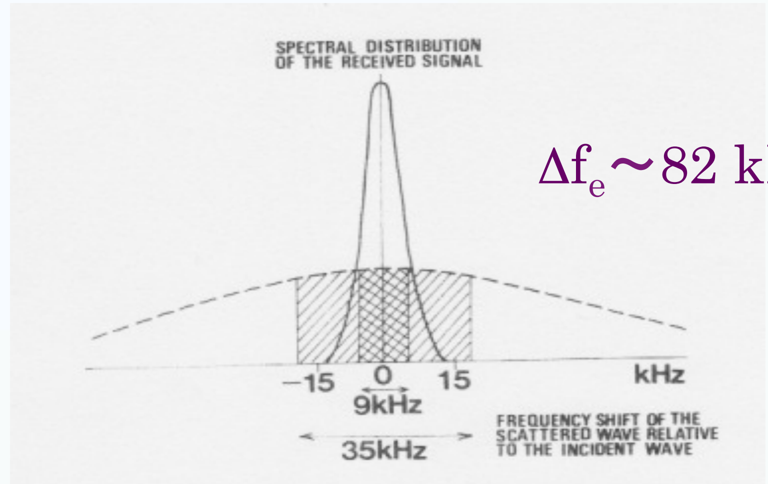

$\Delta f_e \sim 82\ \mathrm{kHz}$

Bowles' Experiment (1958)

RADAR PULSES: $f = 40.92\ \mathrm{MHz}$
width $120\ \mu\mathrm{s}$ $\gg f_p = 13\ \mathrm{MHz}$
repetition $25\sim 40\ \mathrm{s}^{-1}$ $\Delta f = 9\ \mathrm{kHz}$
peak power: $1\ \mathrm{MW}$

Pineo et al's Experiment (1960)

$f = 440\ \mathrm{MHz}$

$k \ll k_D \sim 5.3\ \mathrm{cm}^{-1}$
collective motion!!

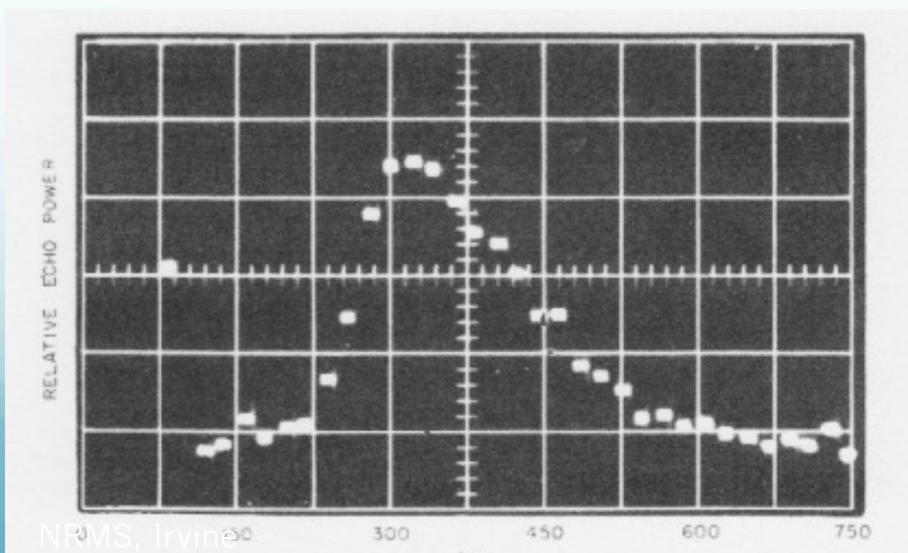

vertical density profile

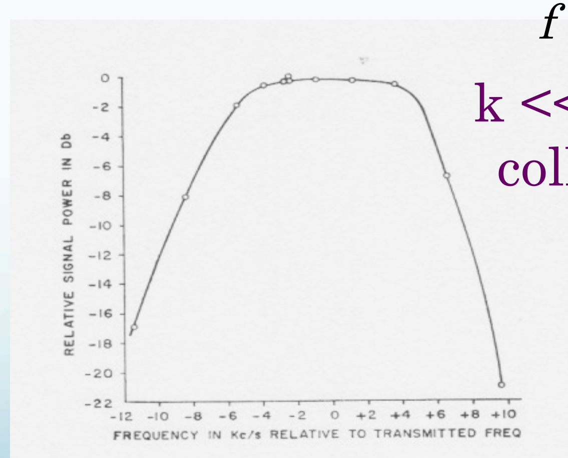

Scattering by electrons co-moving with ions, or by "dressed" ions!

PLASMA CRITICAL OPALESCENCE

Scattering of electromagnetic waves by electron density fluctuations associated with an onset of acoustic-wave instability due to drift motion V_d of electrons relative to ions

$$S = \sim V_i \, (T_e/T_i)^{1/2} : \text{ion-acoustic velocity}$$

ION-ACOUSTIC WEAVE : $\omega_k = s\,k$

a well-defined excitation, when $T_e >> T_i$; for $k < k_D$

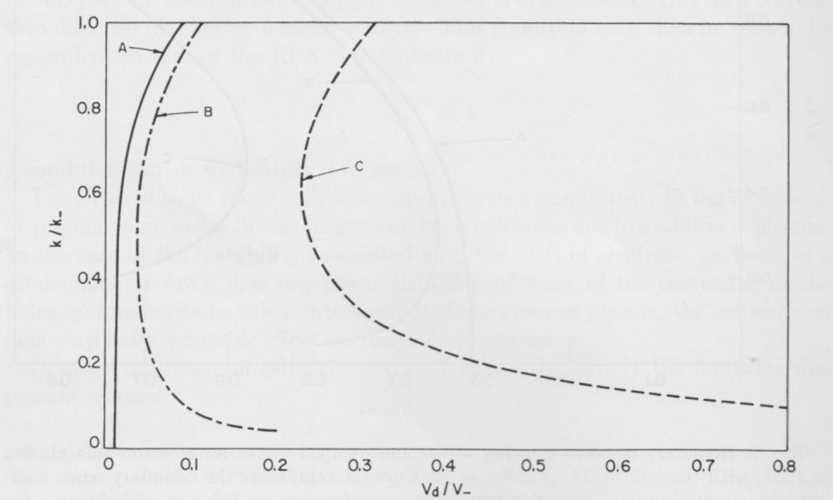

FIG. 4. Boundary between growing waves and damped waves for a helium plasma with $(m_+/m_-) = 4 \times 1836$, $(T_-/T_+) = 20$. Curve A represents the boundary when ion short-range collision is neglected, curve B the case for $\omega_+\tau_+ = 100$, curve C the case for $\omega_+\tau_+ = 10$; τ_+ is the relaxation time of ions due to short-range collision.

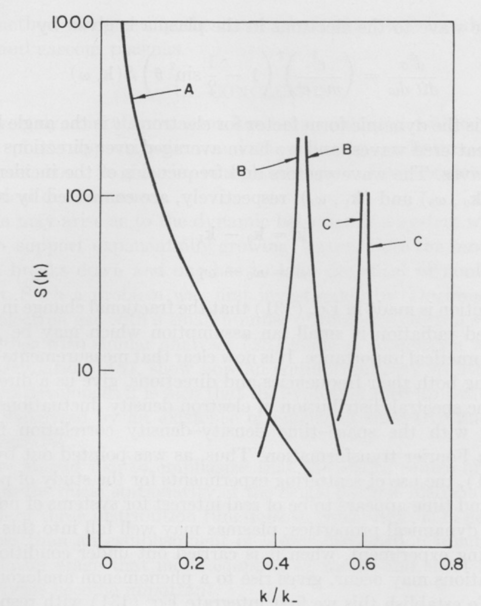

. The form factor $S(k)$ at the critical point, $V_d = V_c$ for $\cos\chi = 1$ and the

STATIC STRUCTURE FACTOR

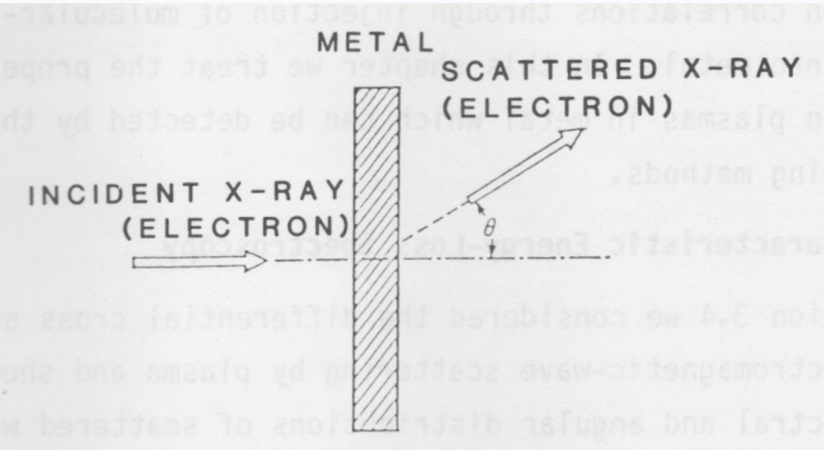

$$\frac{1}{n}\int_{-\infty}^{\infty} d\omega\, S(\mathbf{k},\omega) = S(\mathbf{k})$$

$$S(\mathbf{k}) = \frac{1}{N}\left\langle |\rho_{\mathbf{k}}(t)|^2 \right\rangle = \frac{1}{N}\left\langle \rho_{\mathbf{k}}(t)\rho_{-\mathbf{k}}(t) \right\rangle$$

Spectral distribution of spatial density fluctuations or spatial configurations of density distribution such as lattice structures

$$\mathrm{d}Q/\mathrm{d}o = (3N/8\pi)\,\sigma_{\mathrm{T}}\,(1 - 0.5\,\sin^2\theta)\,S(\mathbf{k})$$

Observation of Laue patterns (1914: M. von Laue) ⇔ X-ray crystallography (1915: W. H. Bragg & W. L. Bragg)

Short-ranged crystalline order at the nearest-neighbor separations

Observation of Layered Structures and Laue Patterns in Coulomb Glasses

Shuji Ogata and Setsuo Ichimaru
Department of Physics, University of Tokyo, Bunkyo-ku, Tokyo 113, Japan
(Received 5 October 1988)

We report the first observation of layered structures in the computer-simulated Coulomb glasses produced by rapid quenching of one-component plasmas in the absence of an external force field. Degrees of polycrystalline nucleation and the nature of local order developed in the glasses are elucidated through analyses of the intralayer and interlayer particle correlations and by means of the Laue patterns formed by scattering of plane waves. Stages of evolution for the glass transition in Coulombic systems are conjectured.

Γ: Coulomb coupling parameter for a one-component plasma (OCP)

$$\Gamma = \frac{(Ze)^2/a}{k_B T} = 2.69 \times 10^{-5} Z^2 \left[\frac{n}{10^{12}\ \mathrm{cm}^{-3}}\right]^{1/3} \left[\frac{T}{10^6\ \mathrm{K}}\right]^{-1}$$

Dynamic evolution and formation of Coulomb glasses by the Monte Carlo simulation method, starting with equilibrated fluid state at Γ = 160

Probability of acceptance for the Monte Carlo configurations generated by random displacements of particles

$$P = \begin{cases} \exp\left(-\dfrac{\Delta E}{k_B T}\right), & \text{if } \Delta E > 0, \\ 1, & \text{if } \Delta E \le 0, \end{cases}$$

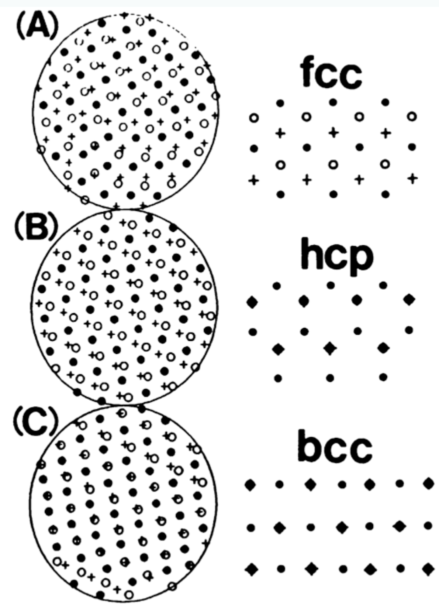

FIG. 2. Normal projections of most closely packed layers: open circles, upper layer; closed circles, middle layer; crosses, lower layer.

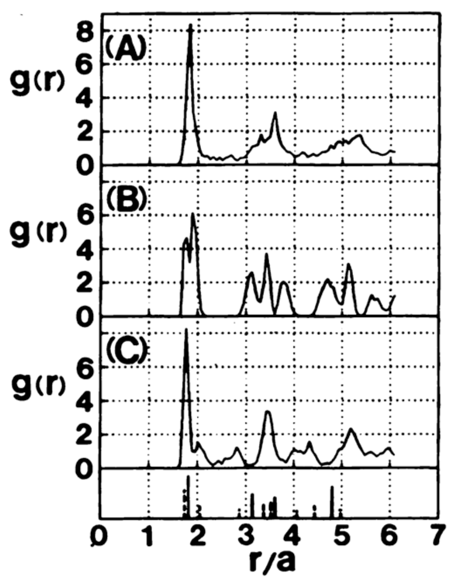

FIG. 4. Two-dimensional radial distribution functions between intralayer particles in the glasses (A)–(C). The bottom of the figure shows the peak positions for the fcc-hcp (solid lines) and bcc (dashed lines) lattices.

fcc = face-centered cubic st.
hcp = hexagonal close-packed st.
bcc = body-centered cubic st.

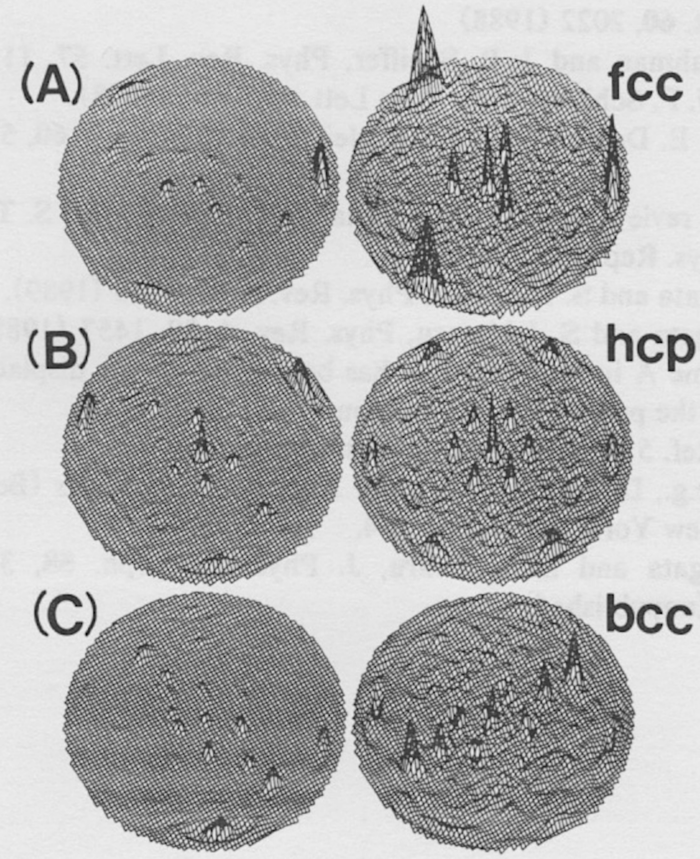

FIG. 5. Laue patterns for the glasses (A)–(C) and for the fcc, hcp, and bcc lattices of 432 particles. The polar coordinates consist of $0 \le (\pi - \chi)/2 \le 0.45\pi$ and $0 \le \phi \le 2\pi$; the origin corresponds to $\chi = \pi$.

(A) sudden quench to $\Gamma = 400$
(B) gradual quench stepwise with $\Delta\Gamma = 10$ from $\Gamma = 160$ at c = 0 to $\Gamma = 400$ at c = 2.3 x 10^7 configurations
(C) sudden quench to $\Gamma = 300$

χ = the scattering angle between $\mathbf{k}_1$ and $\mathbf{k}_2$
ϕ = the azimuthal angle around $\mathbf{k}_1$

Penning-trapped, laser-cooled, strongly coupled, non-neutral ion plasma

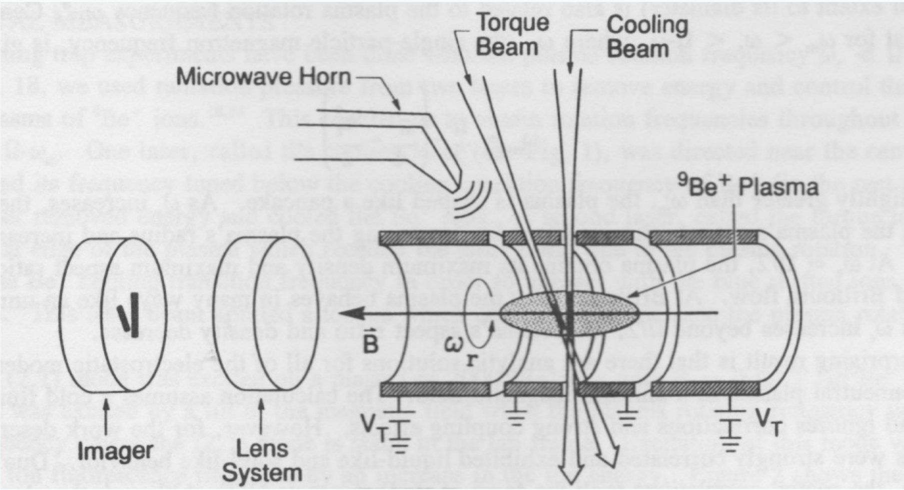

Penning trap

J. Bollinger and D. Wineland: *PRL* **53**, 348 (1984)

a non-neutral OCP in the co-rotating frame of reference – can be maintained stably for many hours

$n = 2\sim 3\text{x}10^7$ cm^{-3}

$Tc = 10\sim 60$ mK, $Tz = 70\sim 150$ mK

$\Gamma = 5\sim 10$

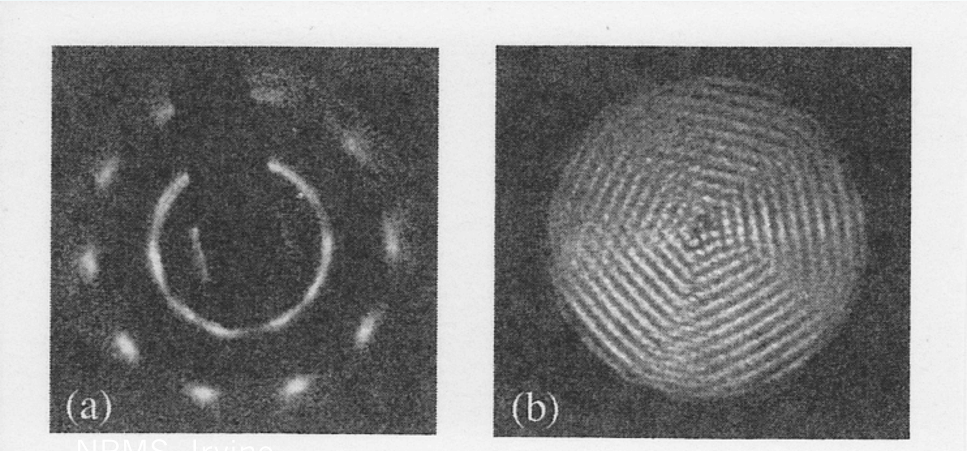

5-fold symmetry exhibited in Laue pattern with ultra-cold $1.2\text{x}10^5$ $^9Be^+$ ions (1999)

(a) Bragg signal in k-space

(b) CT scan picture for 4 layers of ion configuration

"ionic quasi-crystals?"

Collective vs. Individual Particles Aspects of Fluctuations

Bohm-Pines Theory (1951～1953) of "A Collective Description of Electron Interactions"

The density fluctuations may be split into two approximately independent components. The collective component, that is, the plasma oscillation, is present only for wavelengths greater than the Debye length. The individual particles component represents a collection of individual electrons surrounded by co-moving clouds of screening charges; collisions between them may be negligible under the random-phase approximation (RPA).

1. Collective Mode

Dielectric response function: $\varepsilon\,(\mathbf{k},\omega)$

$$\varepsilon\,(\mathbf{k},\omega) = 0 \quad \Rightarrow \quad \omega = \omega\,(\mathrm{k}) - i\,\gamma\,(\mathrm{k})$$

Individual Electrons

$$\mathbf{r}_{\mathrm{j}}\,(t) = \mathbf{r}j + \mathbf{v}_{\mathrm{j}}\,t$$

$$\rho_j^{(0)}(\mathbf{k},\omega) = 2\pi\,\exp\,(-i\mathbf{k}\cdot\mathbf{r}_j)\,\delta(\omega - \mathbf{k}\cdot\mathbf{v}_j)\,.$$

2. Dressed Electrons

$$\rho_j^{(S)}(\mathbf{k},\omega) = \frac{\rho_j^{(0)}(\mathbf{k},\omega)}{\varepsilon\,(\mathbf{k},\omega)}\,.$$

RPA Structure Factors

Superposition of Dressed Test Charges (Rostoker and Rosenbluth, 1960; Ichimaru, 1962)

$$S(\mathbf{k},\omega) = \frac{S^{(0)}(\mathbf{k},\omega)}{|\,\varepsilon(\mathbf{k},\omega)\,|^2},$$

$$S^{(0)}(\mathbf{k},\omega) = \int d\mathbf{p} F(\mathbf{p}) \delta(\omega - \mathbf{k}\cdot\mathbf{v})$$

$$S^{(0)}(\mathbf{k},\omega) = \frac{n}{k}\sqrt{\frac{m}{2\pi T}}\exp\left(-\frac{m\omega^2}{2Tk^2}\right)$$

RADIAL DISTRIBUTION FUNCTION and CORRELATION ENERGY

$$g(\mathbf{r}) = 1 + \frac{1}{n}\int \frac{d\mathbf{k}}{(2\pi)^3}[S(\mathbf{k}) - 1]\exp(i\mathbf{k}\cdot\mathbf{r}).$$

radial distribution function = a joint probability density of finding two particles at a separation r

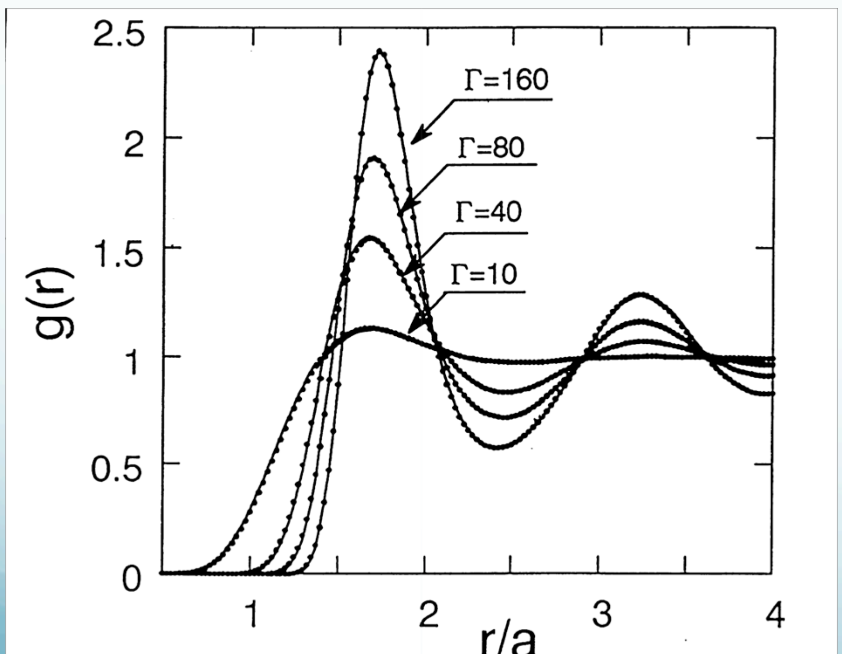

Coulomb correlation energy

$$U_{\text{int}} = 2\pi(Ze)^2 n \int \frac{d\mathbf{k}}{(2\pi)^3}\frac{1}{k^2}[S(\mathbf{k}) - 1]$$

$$= \frac{(Zen)^2}{2}\int d\mathbf{r}\,\frac{1}{r}[g(\mathbf{r}) - 1].$$

RPA internal energy density

$$\frac{U}{nk_BT} = \frac{3}{2} - \frac{\sqrt{3}}{2}\,\Gamma^{3/2} \qquad (\Gamma \ll 1)$$

kinetic + Debye-Hückel

MULTI-PARTICLE CORRELATION and OCP INTERNAL ENERGY

$$u_{\rm ex}^{\rm ABE} = -\frac{\sqrt{3}}{2}\Gamma^{3/2} - 3\Gamma^3\left[\frac{3}{8}\ln(3\Gamma) + \frac{\gamma}{2} - \frac{1}{3}\right],$$

$(\Gamma < 0.1)$

$\gamma = 0.57721\cdots$ Euler's constant

- giant cluster expansion calculation (Abe, 1959)
- expansion in Γ of the BBGKY hierarchy (O'Neil and Rostoker, 1965)
- multiparticle correlation in the convolution approximation (Totsuji and Ichimaru, 1973)
- density-functional formulation of multi-particle correlations (Ichimaru, Iyetomi and Tanaka, 1987 - review)

$$u_{\rm ex}^{\rm OCP}(\Gamma) = -0.898004\Gamma + 0.96786\Gamma^{1/4} + 0.220703\Gamma^{-1/4} - 0.86097\,.$$

$(1 < \Gamma < 180)$

- Monte Carlo simulations (Slattery, Doolen and DeWitt, 1982; Ogata and Ichimaru, 1987)

$$\boxed{u_{\rm ex}(\Gamma) = \frac{u_{\rm ex}^{\rm ABE}(\Gamma) + (3\times 10^3)\Gamma^{5.7}u_{\rm ex}^{\rm OCP}(\Gamma)}{1 + (3\times 10^3)\Gamma^{5.7}}\,.}$$

$(\Gamma < 180)$

Equations of State for the Metallic Hydrogen

Metallic fluid = itinerant electrons (fermions with spin ½) and itinerant protons (classical, or fermions with spin ½) with strong e-i coupling

Metallic solid = itinerant electrons (fermions with spin ½) and a body-centered cubic (bcc) array of protons (classical) with harmonic and anharmonic lattice vibrations and with strong e-i coupling

Fluid-solid transitions ⇔ comparison of the Gibbs free energy: $G = F + PV$; at a constant pressure: $P = -(\partial F/\partial V)_T$

Equations of State for an Insulator Phase of Hydrogen

Molecular fluid = an ideal Bose gas, short-range repulsive interaction between molecular cores, attractive (dipolar) van der Waals forces, molecular rotation (roton), intramolecular vibration (vibron), and the ground-state energy of a H2 molecule ($E_{\mathrm{H_2}}$)

Molecular solid = cohesive energy with a hexagonal-close-packed structure, lattice vibration (phonon), roton, vibron, and the ground-state energy of a H2 molecule ($E_{\mathrm{H_2}}$)

Fluid-solid transitions:

$$P_{\mathrm{mol.fl.}}(\rho_{\mathrm{fl}}, T) = P_{\mathrm{mol.sol.}}(\rho_{\mathrm{sol}}, T)$$
$$G_{\mathrm{mol.fl.}}(\rho_{\mathrm{fl}}, T) = G_{\mathrm{mol.sol.}}(\rho_{\mathrm{sol}}, T)$$

Equations of State for Atoms and Molecules

Mixture of atomic and molecular fluid

$$f_{\mathrm{at.mol.fl}} \equiv \frac{F_{\mathrm{at.mol.fl}}}{N_{\mathrm{H}} k_{\mathrm{B}} T}$$

$$= \frac{n_{\mathrm{m}}}{n_{\mathrm{H}}} \left(f_{\mathrm{m}}^{\mathrm{id}} + f_{\mathrm{rot}} + f_{\mathrm{vib}} + \frac{E_{\mathrm{H_2}}}{k_{\mathrm{B}} T} \right)$$

$$+ \frac{n_{\mathrm{a}}}{n_{\mathrm{H}}} \left(f_{\mathrm{a}}^{\mathrm{id}} + \frac{E_{\mathrm{H}}}{k_{\mathrm{B}} T} \right)$$

$$+ \frac{n_{\mathrm{m}} + n_{\mathrm{a}}}{n_{\mathrm{H}}} (f_{\mathrm{HS}} + f_{\mathrm{attr}}),$$

E_{H2} = the ground-state energy of a H_2 molecule

Equations of State for Hydrogen

H. Kitamura and S. Ichimaru, J. Phys. Soc. Jpn **67**, 950 (1998)

$$
\begin{aligned}
f_{\mathrm{tot}}(n_{\mathrm{H}}, T; \langle Z\rangle, \alpha_{\mathrm{d}}) &\equiv \frac{F}{N_{\mathrm{H}} k_{\mathrm{B}} T} \\
&= \frac{(1-\alpha_{\mathrm{d}})(1-\langle Z\rangle)}{2}\left(f_{\mathrm{m}}^{\mathrm{id}} + f_{\mathrm{vib}} + f_{\mathrm{rot}} + \frac{E_{\mathrm{H}_2}}{k_{\mathrm{B}}T}\right) \\
&\quad +\alpha_{\mathrm{d}}(1-\langle Z\rangle)\left(f_{\mathrm{a}}^{\mathrm{id}} + \frac{E_{\mathrm{H}}}{k_{\mathrm{B}}T}\right) + \langle Z\rangle f_{\mathrm{met.fl}}(\bar{n}, T) \\
&\quad + \frac{(1+\alpha_{\mathrm{d}})(1-\langle Z\rangle)}{2}(f_{\mathrm{HS}} + f_{\mathrm{attr}}).
\end{aligned}
$$

molecular

atomic

metallic

mixture

At a given n_{H} and T, the chemical equilibrium may be achieved through the conditions that f_{tot} be minimized with respect to <Z> and α_{d}, the degrees of ionization and dissociation.

Metal-Insulator Transitions

$$
\begin{aligned}
P(\rho_{\mathrm{M}}, T) &= P(\rho_{\mathrm{I}}, T), \\
G(\rho_{\mathrm{M}}, T) &= G(\rho_{\mathrm{I}}, T).
\end{aligned}
$$

Metal-Insulator Transitions in Dense Hydrogen: Equations of State, Phase Diagrams and Interpretation of Shock-Compression Experiments

Hikaru KITAMURA and Setsuo ICHIMARU[1]

Institute for Solid State Physics, University of Tokyo, Minato-ku, Tokyo 106
[1] *Department of Physics, University of Tokyo, Bunkyo-ku, Tokyo 113*

(Received September 12, 1997)

First-principles formulations of the equations of state for hydrogen in metallic and insulator phases are presented, leading to a phase diagram predicting *first-order* metal-insulator transitions in dense hydrogen. The theory explicitly takes into account the effects of strong electron-ion coupling near the transitions as well as those of lowering or elimination of the atomic and/or molecular levels due to plasma screening. It is shown that the results of recent shock-compression experiments prove consistent with such first-order insulator-to-metal transitions. These observations predict a discontinuous distribution of density and resistivity with a large magnetic Reynolds number near the Jovian surface; the latent heat through the metal-to-insulator transitions is estimated.

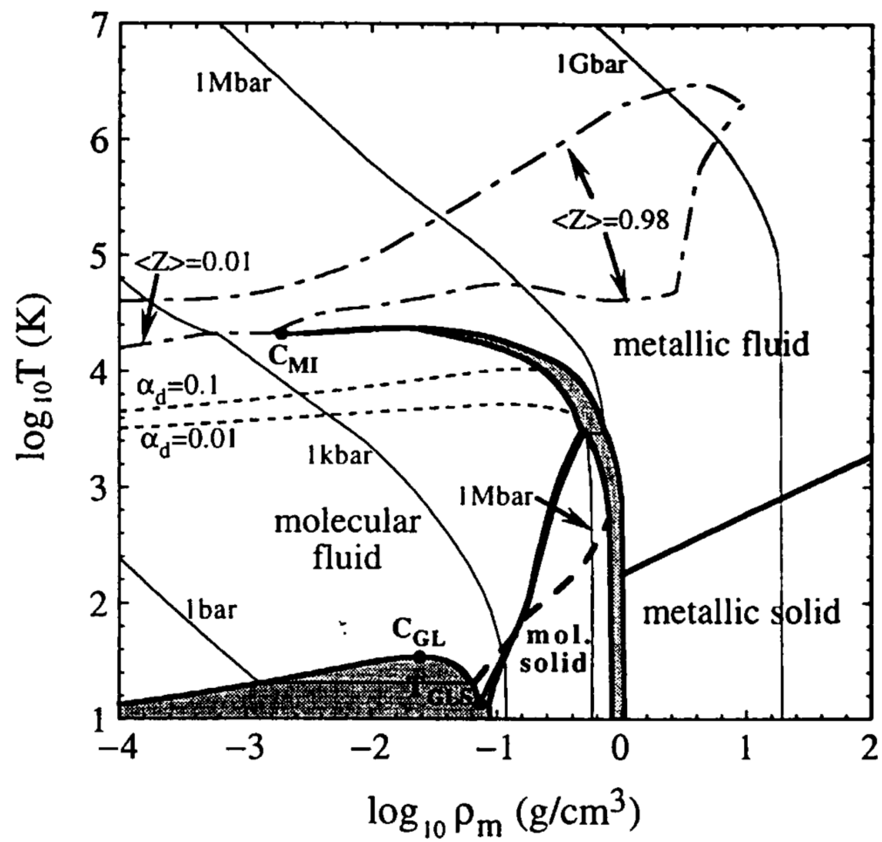

Fig. 1. Phase diagram of hydrogen. C_{MI} and C_{GL} denote the critical points of the metal-insulator and the gas-liquid transitions, respectively; T_{GLS} is the gas-liquid-solid triple point. The solid curves depict the isobars at the designated pressure values. The thick dashed curve represents the isentrope starting from (20 K, 1 bar).

Metallic fluid and solid = itinerant electrons (fermions with spin ½) and itinerant or body-centered cubic (bcc) array of protons (classical)

Molecular fluid and solid hydrogen

Mixture of atomic and molecular hydrogen

PHASE DIAGRAM OF HYDROGEN

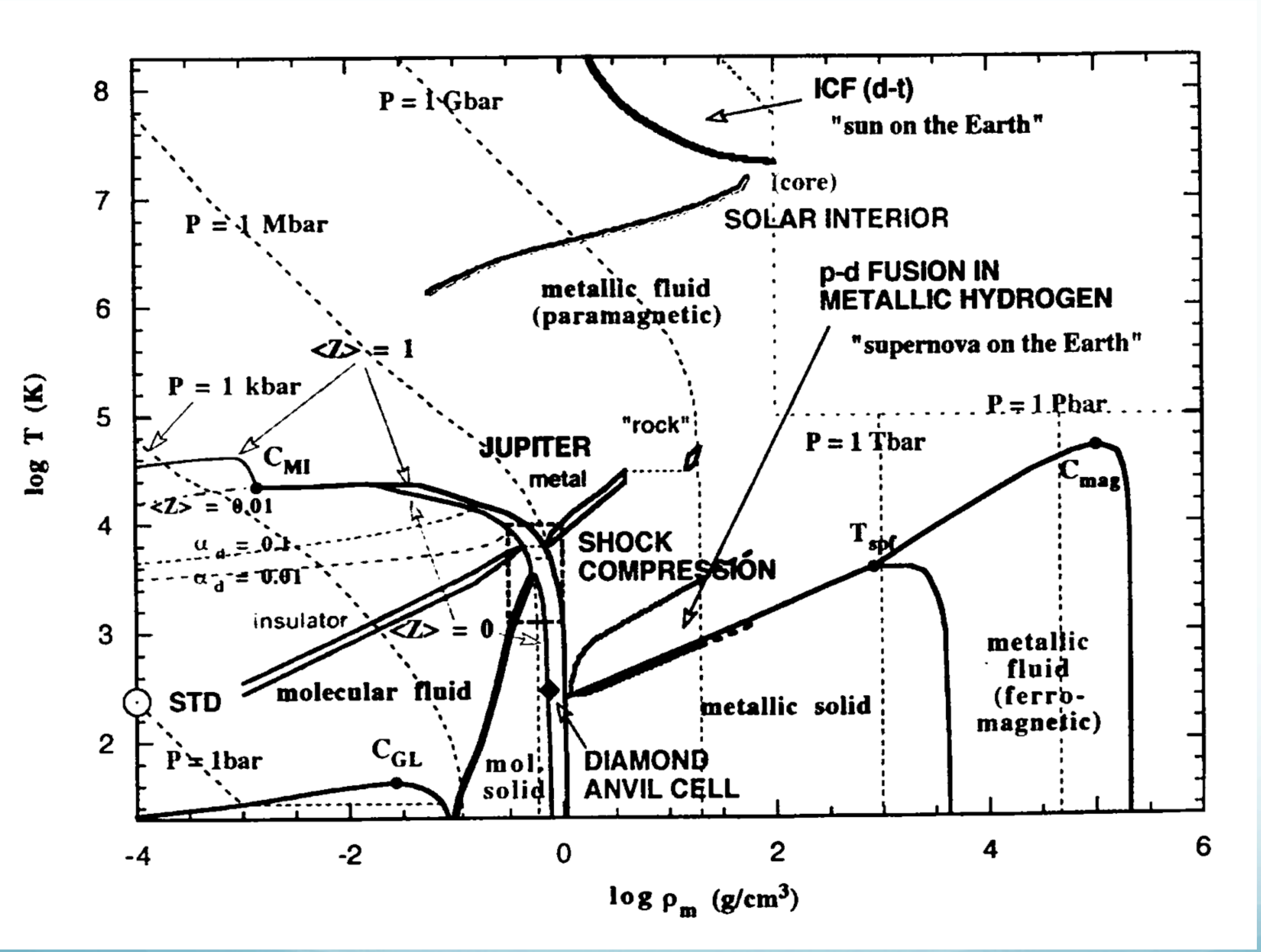

PROTONS

fermions with spin ½
in the ground state

Based on: H. Kitamura and S. Ichimaru, J. Phys. Soc. Jpn **67**, 950 (1998)

Magnetization and Solidification of Metallic Hydrogen

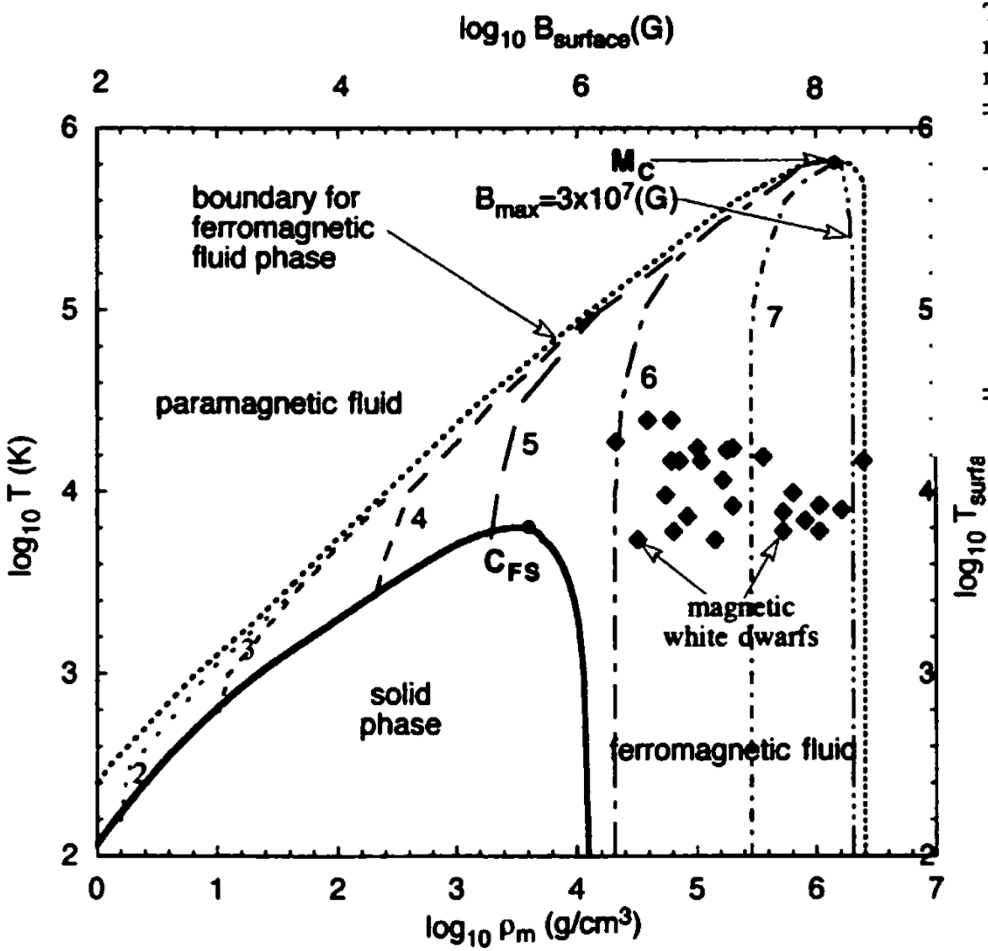

TABLE I. Physical parameters at the fluid–solid critical point (C_{FS}) and the magnetic critical point (M_C) in the phase diagrams of Fig. 1 for the liquid-metallic hydrogen.

	C_{FS}	M_C
ρ_m (g/cm^3)	4.0×10^3	1.4×10^6
R_s	161	22.4
T (K)	6.6×10^3	6.6×10^5
Θ	0.159	0.317
B_M (G)	2.6×10^5	8.0×10^6
Γ_s	517	34.4

magnetic Reynolds numbers for intensification of magnetic field

$$R_m \equiv \frac{4\pi R_{WD}^2 \omega_{WD}}{\rho_E c^2} \approx 3.8\times10^{16}\left(\frac{R_{WD}}{5000\ \mathrm{km}}\right)^2\left(\frac{\omega_{WD}}{2\pi/\mathrm{day}}\right),$$

$\sim 1.2 \times 10^{12}$ (Jovian activities)
$\sim 1.0 \times 10^{8}$ (solar activities)

S. Ichimaru, Phys. Plasmas **8**, 48 (2001)

Phase Diagram of Nuclear Matter

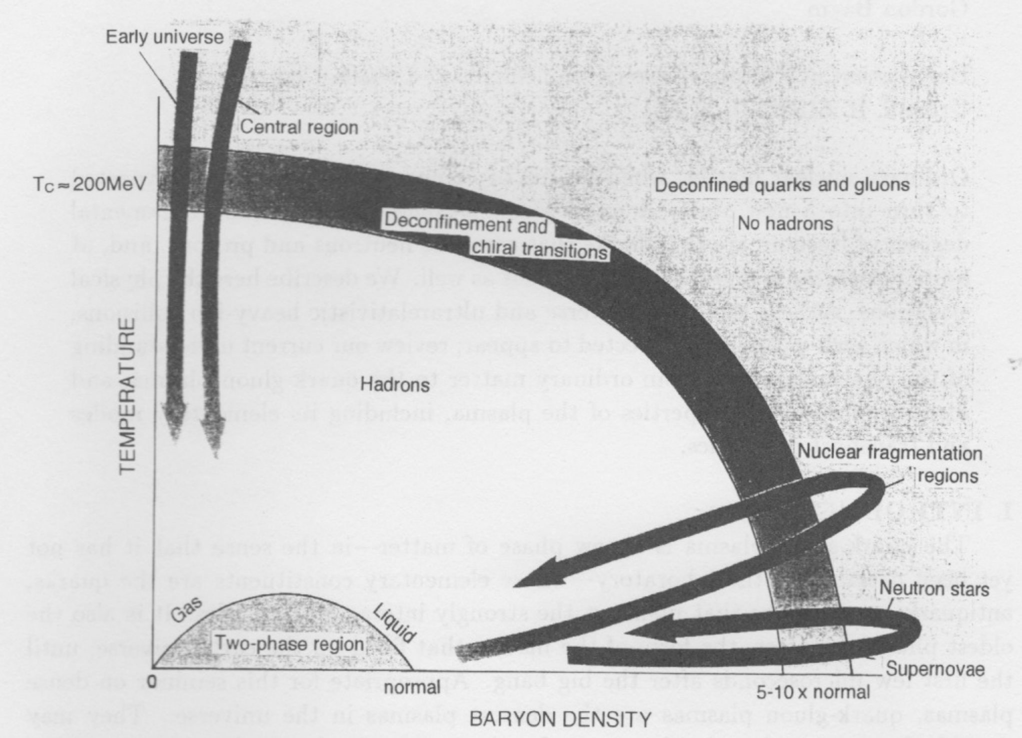

Figure 1. Phase diagram of equilibrated nuclear matter in the baryon density, temperature plane. [Baym]

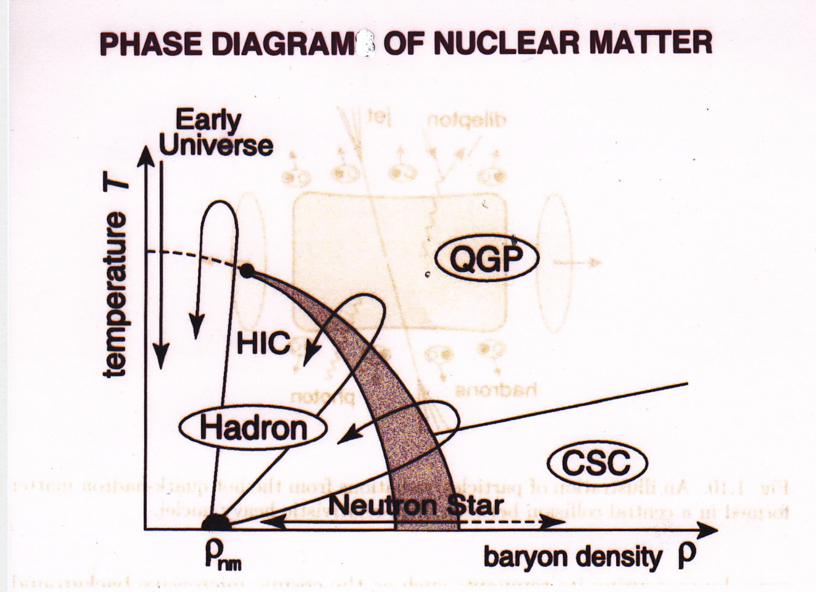

From K. Yagi, T. Hatsuda & Y. Miake "QUARK-GLUON PLASMA"

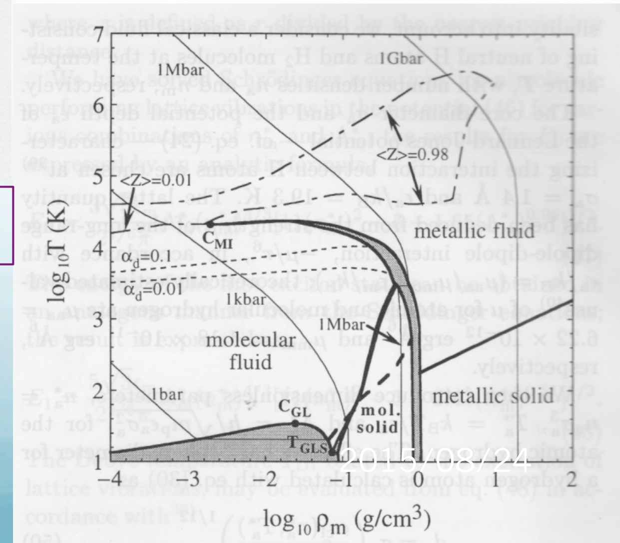

deconfinement of quarks ⇔ metallization

hadrons — insulators

quark gluon plasmas — metals

Concluding Remark

It is clear from what we have surveyed on the two subjects:

"Scattering of Electromagnetic Waves by a Strongly Correlated Plasma"

and

"Multi-particle Correlation, Equations of State, and Phase Diagrams"

that Norman Rostoker made outstanding contributions to the advancement of the fundamental plasma physics.